EELWORM: a bioinspired multimodal amphibious soft robot

Edoardo Milana[1], Bert Van Raemdonck[1], Kevin Cornelis, Enrique Dehaerne, Jef De Clerck, Yarno De Groof, Toon De Vil, Benjamin Gorissen[1,2] and Dominiek Reynaerts[1]

***Abstract*— Exploration robots are challenged by a continuous adaptation to the terrain induced by ever changing environments. These adaptations can be subtle (e.g. when moving from a smooth to a rough terrain), however drastic changes in environment require robots to address different locomotion modes (e.g. crawling vs swimming). While each locomotion mode can be driven by a dedicated set of actuators, nature shows that multimodal locomotion is also possible by activating the same set of actuators in different sequences (e.g. swimming snakes). In this paper, we present EELWORM, a 40 cm long soft-bodied robot consisting out of an arrangement of five inflatable bending and elongating actuator modules that can be addressed individually. EELWORM is capable of both crawling and swimming by varying the actuation sequences within the same embodiment. We show multimodal locomotion at speeds of 2 body lengths per minute (crawling) and 3 body lengths per minute (swimming).**

I. Introduction

Soft robots are foreseen to have a big impact in applications that are characterized by unpredictable interactions with the environment. Particular focus areas include rehabilitation robots and robots for minimally invasive surgery where the human is the unpredictable factor and softness is used to ensure inherent safety [1]. Another application in which soft robots could be deployed is search and rescue (SAR) activities [2]. Here a high level of compliance makes it possible to navigate unstructured environments without having complete information about them [3]. And ideally, an exploratory robot needs to be able to operate in a large variety of such environments by adapting its shape and locomotion pattern accordingly.

Research into soft SAR robots eventually aims at highly adaptable robots that can cope with any environment. However, an important intermediate milestone in the roadmap towards that goal is a framework for soft robots that can switch between a predetermined set of two completely different environments. In this paper we have chosen these environments to be water and land.

Regarding terrestrial locomotion of entirely soft robots, crawling is the most researched type of motion. Trimmer et al. pioneered the field with a caterpillar-like limbless soft robot (GoQBot) actuated through SMA coils [4]. Shepherd et al. made a soft-bodied quadruped composed of five inflatable bending actuators performing multiple gait patterns depending on the inflation sequence [5]. More recently, a robot with three elongating segments mimicking euglenoid movement has been designed with the ability to navigate an unknown environment [6]. Duggan et al. [7] proposed an inchworm-like autonomous soft robot composed of three segments, each comprising two inflatable bending actuators, to direct the crawling motion. Rafsanjani et al. proposed a soft robot made out of a single inflatable actuator wrapped with a kirigami skin [8]. The mechanical instability occuring in the kirigami skin induces differential friction that creates locomotion even when the actuator is inflated in a time-symmetric sequence.

From the aquatic locomotion side, there are different approaches, each inspired by a different animal. PoseiDRONE, an octopus-like soft robot, uses a water jet for propulsion and four tentacles for manipulation and seabed crawling [9]. The untethered jellyfish soft robot by Frame et al. swims vertically and steers thanks to eight pneumatic bending actuators placed around a ring [10]. MITs soft robotic fish swims through undulation generated by the alternating inflation of two hydraulic chambers in the tail [11].

It is important to note that each of these robots was precisely designed to operate in a specific environment (land or water). If they would be placed in a radically different environment, they would be rendered useless. Many organisms do not suffer this limitation, however. Depending on their perceived environment, humans can adapt the actuation sequence of their limbs to change their mode of locomotion from walking to jumping, crawling, climbing or swimming. And despite numerous examples in hard-bodied robotics [12][13], there are still very few reports on soft-bodied robots with similar multimodal locomotion capabilities.

At a small-scale, it has been shown that a magnetic-elastic soft robot can swim, crawl and roll in different environments, even if its operation is limited by the range of the driving magnets [14]. On a larger scale, Baines et al. designed a morphing limb that adapts to land and water locomotion for use in amphibious soft robots [15].

In this paper we propose a new design for a compact soft-bodied robot capable of multimodal amphibious locomotion. A bioinspired inchworm-like gait is adopted for terrestrial locomotion and anguilliform swimming for aquatic locomotion. This so-called EELWORM robot consists of five elastic inflatable actuators that can be independently pressurized with air. The design is a serial connection of bending and elongating modules that function both as actuators and structural elements. By tuning their distributed stiffness and frictional properties, both swimming and crawling speeds are

*This research is supported by the Fund for Scientific Research-Flanders (FWO). Corresponding author: edoardo.milana@kuleuven.be

All authors are with the Department of Mechanical Engineering, KU Leuven, Leuven, Belgium

[1]These authors are also members of Flanders Make, Belgium

[2]Benjamin Gorissen is also affiliated to John A Paulson School of Engineering and Applied Sciences, Harvard University.

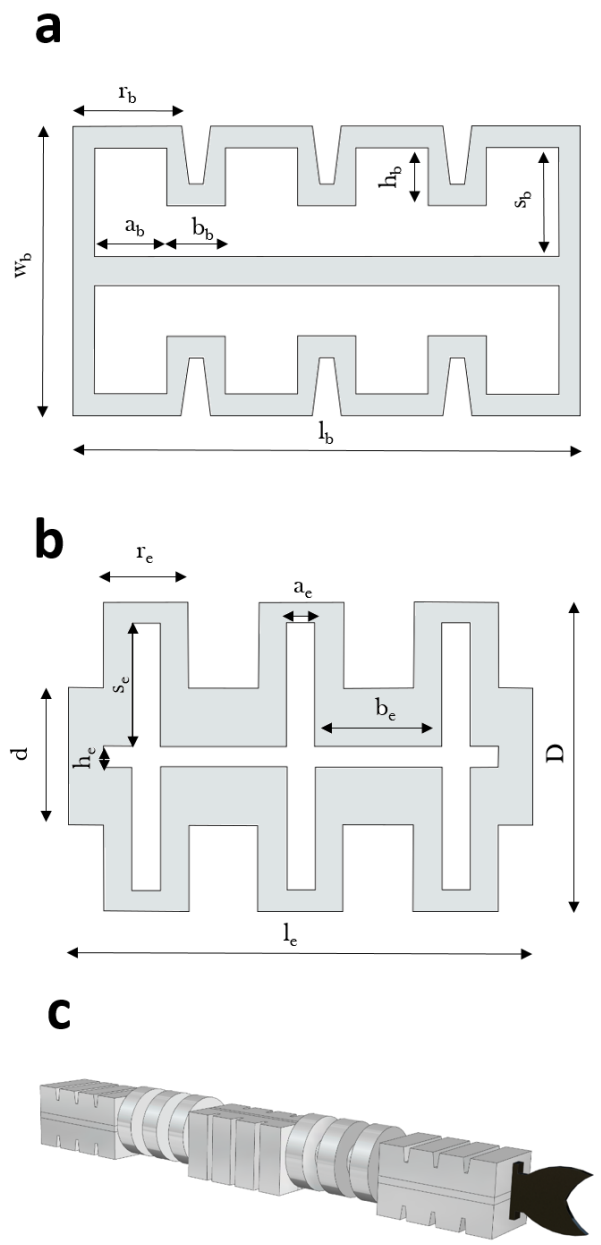

Fig. 1. a) Profile sketch of the bending segment. b) Profile sketch of the extending segment. c) 3-D representation of EELWORM

enhanced.

In the first section the structure of the robot and the design and manufacturing of the actuators are presented. The following section reports on the experimental characterization of the two modules and compares the results to FEM simulations. The final section discusses the multimodal amphibious locomotion pattern of the robot as well as experimental results and morphological changes.

II. Design and Manufacturing

As the name suggests, the multimodal locomotion of EELWORM (EW) is based on the crawling motion of a worm on land and the swimming motion of an eel in water. Earthworms crawl by activating muscles in consecutive segments along their body that lead to simultaneous axial contraction and radial expansion of those segments. Thick, contracted segments experience more friction with the ground than the segments which are lifted off the ground. They will therefore act as anchor points while the other segments elongate without gaining traction against the ground [16]. Anguilliform swimmers like eel advance by a sinusoidal wave motion along their flexible slender body. The undulation is caused by metachronal contraction waves that alternate on the left and right side of the body [17]. To increase the versatility of our bioinspired system, we opted for a design based on the assembly of two types of elastic inflatable actuator (EIA) modules as artificial muscles. EIAs are fluidic-driven soft actuators and can be designed in order to perform basic motions like bending, extension, contraction and twisting [18]. The two building blocks are a bidirectional bending actuator and an elongating actuator. As mentioned in the introduction, the body structure is composed of five segments (Fig. 1c). The two outer segments are bi-directional bending actuators that move up and down in the vertical plane containing the longest primary axis of the robot. The central segment is the same bending actuator rotated such that it moves left and right in the horizontal plane. The outer segments are each connected to the central segment via an elongating actuator. The elongating actuators can be shifted upwards so that they do not contact the ground. All actuator modules are permanently glued together so the robot morphology remains the same for both crawling and swimming.

TABLE I
EELWORM DIMENSIONS

Feature	Value (mm)
Bending segment	
Length (l_b)	70
Width (w_b)	40
Rib length (r_b)	15
Inner cavity length (a_b)	10
Inner groove length (b_b)	8
Inner groove height (h_b)	8
Inner cavity height (s_b)	15
Elongating segment	
Length (l_e)	66
Connecting ring diameter (d)	72
Bellow diameter (D)	44
Rib length (r_e)	12
Inner channel diameter (h_e)	3
Inner channel length (b_e)	18
Inner cavity radius (s_e)	19
Inner cavity length (a_e)	4

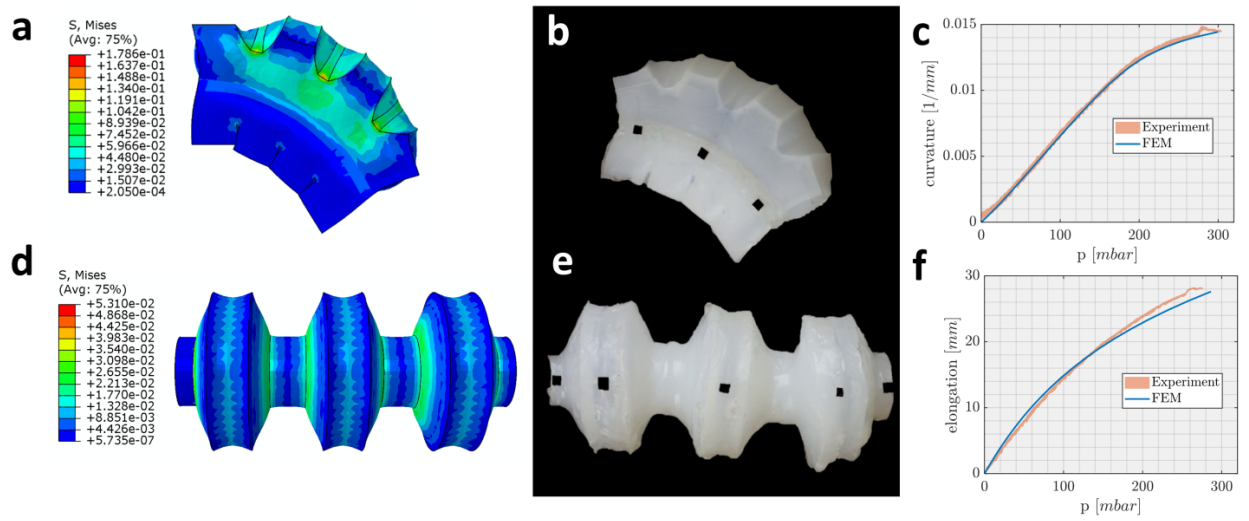

Fig. 2. Actuators characterization. FEM computed Von Mises stress distributions at the operational deformed configuration for the bending a) and the elongating d) actuators. Pictures of the deformed configuration during inflation experiment of the bending b) and elongating e) actuators. Quasi-static experimental vs. FEM simulated characterization of the bending c) and elongating f) actuators

A. Bending actuator

The bidirectional bending actuator (BA) module is a composition of two unidirectional bending segments. Each unidirectional half is based on the design of the PneuNet actuator [19] which features a cavity formed by a corrugated membrane on one side and a layer that is stiff in extension on the other side. Inflating the cavity makes the actuator bend towards the side of the stiffer layer. Connecting two corrugated membranes at opposite sides of a common stiffer layer therefore yields a bidirectional bending actuator. Inflating either cavity and leaving the other one at atmospheric pressure makes the actuator bend towards the unpressurized side.

Bending causes the gaps, which form the corrugations in the membrane, to close at one side. The V-shape of those grooves allows to obtain a certain degree of bending while still operating at low actuation pressures. Fig. 1a depicts a sketch of the BA design and Table I reports the corresponding dimensions.

The actuator is manufactured in three separate parts: a central stiffer layer (70x40x4 mm) made out of silicone rubber, Dragon Skin 30 (Smooth-On), and two identical outer shells made out of a softer rubber, Dragon Skin 20 (Smooth-On). All pieces are glued together with uncured silicone. The mold of the stiffer layer is cut out of MDF wood with a laser cutter. The two outer pieces both come from the same 3D-printed mold featuring four pneumatic cavities. For the rest of the manuscript we refer to the protrusions between the grooves as the ”ribs” of the robot.

B. Elongating actuator

The elongating actuator (EA) module consists of three cylindrical bellows axially connected with soft rings featuring a central air channel. The connecting rings decrease the radial deformation on inflation, which avoids contact with the ground on crawling. They also decrease the bending stiffness of the actuator which increases swimming speeds, as discussed later on. The bellows feature a large cylindrical cavity which expands on inflation. Each bellow is made by attaching two identical halves together with uncured silicone. The same method is used to attach the bellows to the connecting rings, one at each side of every bellow. Both bellows and connecting rings are made of Dragon Skin 20 (Smooth-On) cured in 3D-printed molds. Figure 1b depicts a sketch of the elongating actuator, whose dimensions are reported in Table I.

In all manufacturing processes, Dragon Skin prepolymers are mixed in a 1:1 ratio, degassed and cured at 60 °C for 1h. After assembly, a hole is made in each cavity and a Luer lock connector is inserted and sealed in place with silicone rubber. This connector forms the connection point between the cavity and the tubing for inflation.

III. Actuators Characterization

The actuator deformations are first evaluated through a static FEM simulation, performed with the commercial code Abaqus. A static pressure ramp is imposed inside the fluidic cavity. The two materials of the actuators (Dragon Skin 20 and 30) are modeled with hyperelastic constitutive relations with the following parameters: Arruda-Boyce model for Dragon Skin 20 (μ = 37 kPa, $\lambda_m = 6.73$) and Ogden model (μ = 75.5 kPa, $\alpha = 5.84$) for DragonSkin 30 [20].

The simulations are validated for a pressure-controlled inflation experiment. The set-up consists of a pneumatic pressure regulating valve (Festo LR-D-7-I-Mini) electronically driven by a servo motor controlled by Arduino. Connections are realized using flexible tubes to minimize the force exerted by the tubes on the actuator. The base of the actuator is clamped into a bench vise. Pressure input ramps up to the targeted value (300 mbar) in 10s. Pressure is continuously

recorded by a transducer (Keller PR-21S) connected to an Arduino board and simultaneously an overhead camera (Nikon 1 V3) captures the actuator deformation using attached markers. Curvature and displacement are measured through an image-analysis code in Matlab. Each test is performed five times. The results of both simulation and experiment are plotted in Fig. 2c-f., where the red coloured area corresponds to the standard deviation of the curvature over the tests.

IV. EELWORM LOCOMOTION PATTERN

For locomotion, individual air chambers are pressurized and depressurized using external on-off valves in a sequence determined by an Arduino microcontroller. Since the robot features eight individual addressable inflatable cavities, there is a large amount of possible actuation sequences and corresponding locomotion patterns. In this work we limit the presentation to a single sequence for crawling and one for swimming. Sequences repeat in a loop until a command is given to switch locomotion pattern or stop the motion. All the valves switch between 0 and 300 mbar (gauge

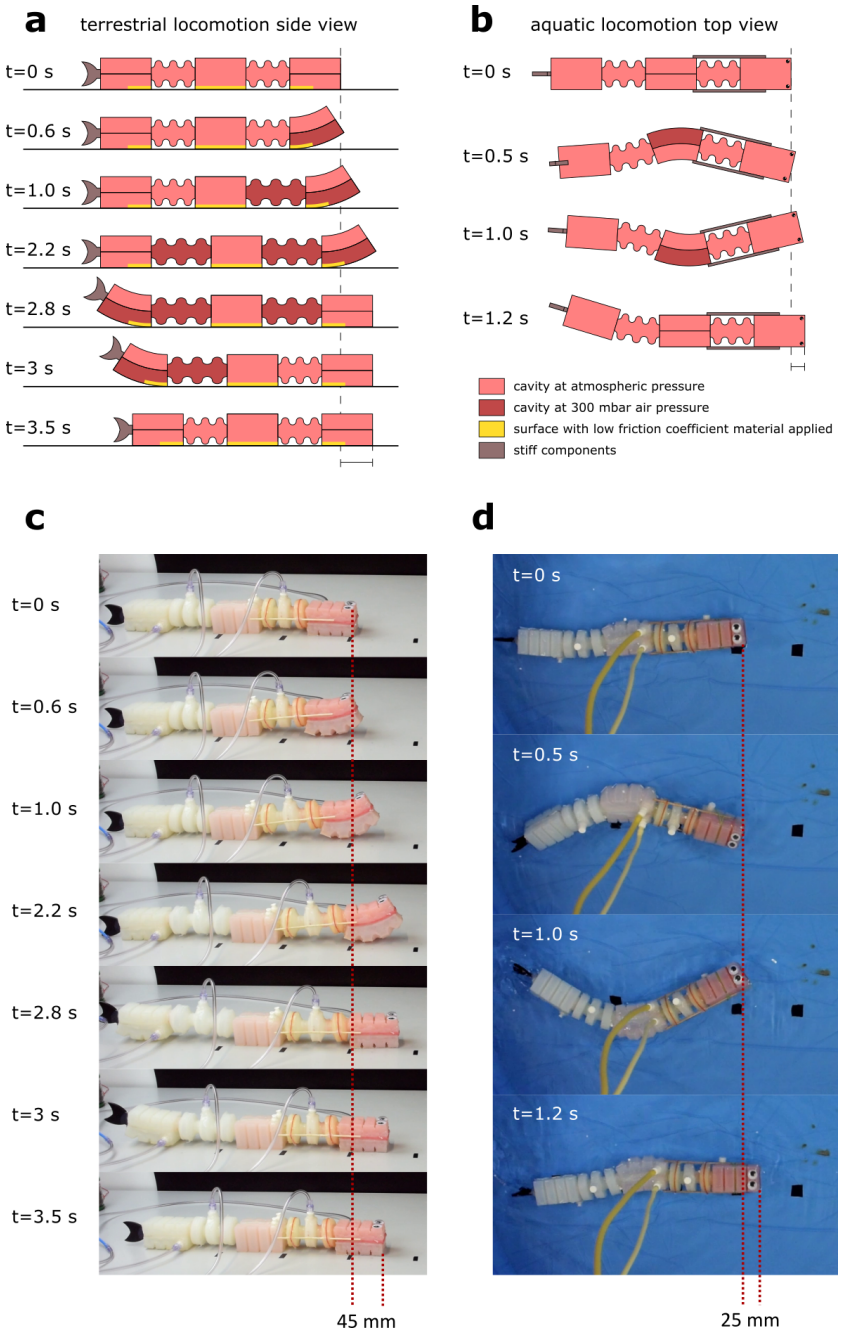

Fig. 3. EELWORM locomotion patterns. Sketches of the actuation sequence for terrestrial locomotion a) and aquatic locomotion b). Video still frames showing EELWORM terrestrial c) and aquatic d) locomotion and relative displacement at end of one actuation sequence cycle.

pressure), which corresponds to the targeted deformation of 0.015 mm^{-1} in curvature (bending actuator) and 28 mm in tip elongation (elongating actuator). Optimization of the different locomotion sequences is a subject for further research.

A. Terrestrial locomotion

In nature, a worm contracts its muscles to thicken part of its body. That anchors the contracted segments down, lifting adjacent segments off the ground so they can translate axially with minimal traction with the ground which could push the body back. This principle is mimicked by the inflation sequence of EW as shown in Fig. 3a. The outer BAs serve as the switchable anchor points, the EAs power the translation and the central BA is passive unless for steering.

In order for the robot to advance rather than expand symmetrically around the center when the elongating actuators are inflated, the difference in friction force between the anchored and unanchored points should be sufficiently high. That asymmetry in friction comes from the shape, surface area, and material of the part of the front and back BA that is in contact with the ground. On inflating the front or back BA, the sharp edges of the actuator bend inwards which decreases friction. Moreover, the two outer ribs are lifted off the ground. A material with a low friction coefficient is applied to the two inner ribs.

The low friction material consist of strips of medical polyethylene tape (3M Transpore), which has a lower coefficient of friction than silicone rubbers for many surfaces [21] and adheres well to silicone rubber. It is attached to both the two inner ribs of the front and back BA and to the entire bottom surface of the central BA to decrease the friction at the center of the robot.

In the inflated state, only the material with low friction coefficient makes contact with the ground while in the deflated state the silicone of the outer ribs provides most of the friction. Both effects contribute to amplify the difference in friction between the inflated (unanchored) and deflated (anchored) state. We calculate the coefficients of friction (COF) of the inflated and deflated state by placing EW on the same surface where the crawling locomotion is tested. Thus, we measure the inclination angle of the surface when EW starts to slip over. The tangent of the angle is used as coefficient of friction, resulting in a value of 0.6 for the deflated state and 0.5 for the inflated state (Table II).

The time needed for the EAs and the BAs to complete the targeted deformation is measured to be 0.6 s on average at 300 mbar gauge pressure. With the polyethylene tape, EW reaches a crawling speed around 45 mm per cycle (compared to 8 mm per cycle without polyethylene tape). Given the total body length of the robot (400 mm) and the time per cycle (3.5 s), the crawling speed is about 2 body lengths per minute in average (fig 3c).

However, due to manufacturing imperfections and asymmetric weight distribution, EW tends to deviate from a straight line trajectory. We repeated 10 crawling cycles for 5 times and measured a trajectory deviation angle of 18.16° in average ($\sigma = 2.25°$).

To calculate the cost of tranport (COT), we filled a 2L aluminium vessel with compressed air at 2 bar and we used it to power a crawling cycle. The theoretical amount of energy stored in a compressed air vessel corresponds to the work required to isothermally fill the vessel volume at the required pressure [22]. Taking into account the atmospheric pressure surrounding the vessel, the formula is:

$$E = PV \ln \frac{P_{atm}}{P} + (P - P_{atm})V \tag{1}$$

By measuring the pressure drop in the vessel we estimate the amount of energy spent using Equation 1. COT is defined by the amount of energy spent, normalized with the product between the weight of the robot and the travelled distance [23].

$$COT = \frac{\Delta E}{mgd} \tag{2}$$

Given the parameters reported in Table II, COT is 316. In future perspectives, this value can be improved by minimizing the energy losses due to long tubing and leakages in the soft actuators. Moreover, the energy released by the soft actuators is currently dissipated by venting the exhaust air to the atmosphere.

B. Aquatic locomotion

Similar to the terrestrial locomotion, the aquatic locomotion needs asymmetric motion to generate net forward motion. In this case the asymmetry arises from differences in water displacement between the front and the back of the robot rather than from differences in friction.

The sequence for this locomotion pattern contains fewer steps than the terrestrial case. It relies exclusively on the oscillatory actuation of the central BA in two directions (fig. 3b) combined with an asymmetric stiffness along the length of the robot. At the tail side, the design of the elongating actuators results in a low bending stiffness towards the tail such that the bending oscillations generated in the central BA are transmitted to the tail of the robot. At the head side, linear guides between the central BA and the front BA increase the bending stiffness in the horizontal plane so the oscillation wave is blocked from travelling to the

TABLE II
TERRESTRIAL LOCOMOTION CHARACTERISTICS

Feature	Value
COF deflated state	0.6
COF inflated state	0.5
EELWORM mass	350 g
Vessel volume	2 L
Mean energy consumption per cycle	48.84 J
SD energy consumption per cycle	1.24 J
Cost of transport (COT)	316

head, resulting in an eel-like undulation. This asymmetry is amplified by incorporating a tail-fin, making the back end of the robot longer than the front without protruding to the bottom to prevent interference with the terrestrial locomotion.

The asymmetry in stiffness and asymmetry in length both increase the amplitude towards the tail side of the robot so that it displaces more water at the back than at the front of the robot. That results in a net forward push with every oscillation of the central BA. The strong decrease in wave motion at the front of the robot has two positive effects. Firstly it dramatically increases the net forward force making the motion much faster and more efficient. Secondly it causes far less uncontrolled directional changes and the robot is able to swim in a straight line. In one cycle (1.2 s) the robot moves 25 mm forward (fig. 3d), resulting in a swimming speed of 3 body lengths per minute in average.

V. Conclusions

EELWORM is a soft-bodied robotic design with multimodal locomotion. The robot is a fixed arrangement of five instances of two basic elastic inflatable modules that function as actuators and structural elements. Terrestrial and aquatic locomotion is achieved through an interplay between actuation sequences and reaction forces coming from the environment. We report a crawling speed around 2 body lengths per minute and a swimming speed around 3 body lengths per minute. More importantly, EW acts as an experimental platform for the final goal of an autonomous, amphibious, soft bodied robot to be deployed in SAR operations. Further research will focus on morphological optimization to increase the undulation amplitude along the body and the frictional difference, without adding other materials. A more precise mould manufacturing process might also correct some current defects that limit soft actuator performances and cause trajectory deviations and energetic inefficiencies. Where in this stage the robot is still tethered, senseless and remotely controlled and powered, in the next step, we aim to transfer the generation of the actuation sequences from the microcontroller to an embodied mechanism, either through a fluidic logic circuit [24][25] or a nonlinear soft fluidic network [26], coupled with a soft water detector sensor for autonomous switching between locomotion types.

Acknowledgment

The authors would like to thank Shashwat Kushwaha, Iago Cupeiro Figueroa and Bert de Jager for their contribution to this work.

References

[1] F. Iida and C. Laschi, "Soft Robotics: Challenges and Perspectives," *Procedia Comput. Sci.*, vol. 7, pp. 99–102, 2011. [Online]. Available:

[2] D. Rus and M. T. Tolley, "Design, fabrication and control of soft robots," *Nature*, vol. 521, no. 7553, pp. 467–475, may 2015. [Online].

[3] R. Pfeifer and G. Gomez, "Morphological computation - Connecting brain, body, and environment," in *Lect. Notes Comput. Sci. (including Subser. Lect. Notes Artif. Intell. Lect. Notes Bioinformatics)*, vol. 5436. Springer, Berlin, Heidelberg, 2009, pp. 66–83.

[4] H. T. Lin, G. G. Leisk, and B. Trimmer, "GoQBot: A caterpillar-inspired soft-bodied rolling robot," *Bioinspiration and Biomimetics*, vol. 6, no. 2, p. 026007, jun 2011.

[5] R. F. Shepherd, F. Ilievski, W. Choi, S. A. Morin, A. A. Stokes, A. D. Mazzeo, X. Chen, M. Wang, and G. M. Whitesides, "Multigait soft robot," *Proc. Natl. Acad. Sci.*, vol. 108, no. 51, pp. 20 400–20 403, 2011.

[6] K. M. Digumarti, A. T. Conn, and J. Rossiter, "Eumobot: Replicating euglenoid movement in a soft robot," *J. R. Soc. Interface*, vol. 15, no. 148, p. 20180301, nov 2018.

[7] T. Duggan, L. Horowitz, A. Ulug, E. Baker, and K. Petersen, "Inchworm-inspired locomotion in untethered soft robots," in *RoboSoft 2019 - 2019 IEEE Int. Conf. Soft Robot.* IEEE, apr 2019, pp. 200–205.

[8] A. Rafsanjani, Y. Zhang, B. Liu, S. M. Rubinstein, and K. Bertoldi, "Kirigami skins make a simple soft actuator crawl," *Sci. Robot.*, vol. 3, no. 15, p. eaar7555, 2018.

[9] A. Arienti, M. Calisti, F. Giorgio-Serchi, and C. Laschi, "PoseiDRONE: design of a soft-bodied ROV with crawling, swimming and manipulation ability," in *2013 Ocean. Diego*. IEEE, 2013, pp. 1–7.

[10] J. Frame, N. Lopez, O. Curet, and E. D. Engeberg, "Thrust force characterization of free-swimming soft robotic jellyfish," *Bioinspiration and Biomimetics*, vol. 13, no. 6, p. 064001, sep 2018.

[11] A. D. Marchese, C. D. Onal, and D. Rus, "Autonomous Soft Robotic Fish Capable of Escape Maneuvers Using Fluidic Elastomer Actuators," *Soft Robot.*, vol. 1, no. 1, pp. 75–87, mar 2014.

[12] A. Crespi, K. Karakasiliotis, A. Guignard, and A. J. Ijspeert, "Salamandra Robotica II: An amphibious robot to study salamander-like swimming and walking gaits," *IEEE Trans. Robot.*, vol. 29, no. 2, pp. 308–320, apr 2013.

[13] R. J. Lock, S. C. Burgess, and R. Vaidyanathan, "Multi-modal locomotion: From animal to application," p. 011001, dec 2014.

[14] W. Hu, G. Z. Lum, M. Mastrangeli, and M. Sitti, "Small-scale soft-bodied robot with multimodal locomotion," *Nature*, vol. 554, no. 7690, pp. 81–85, feb 2018.

[15] R. L. Baines, J. W. Booth, F. E. Fish, and R. Kramer-Bottiglio, "Toward a bio-inspired variable-stiffness morphing limb for amphibious robot locomotion," in *RoboSoft 2019 - 2019 IEEE Int. Conf. Soft Robot.*, 2019, pp. 704–710. [Online].

[16] R. M. N. Alexander, *Principles of animal locomotion*, 2013. [Online].

[17] G. R. Zug, "Locomotion," 2017.

[18] B. Gorissen, D. Reynaerts, S. Konishi, K. Yoshida, J.-W. Kim, and M. De Volder, "Elastic Inflatable Actuators for Soft Robotic Applications," *Adv. Mater.*, p. 1604977, sep 2017.

[19] B. Mosadegh, P. Polygerinos, C. Keplinger, S. Wennstedt, R. F. Shepherd, U. Gupta, J. Shim, K. Bertoldi, C. J. Walsh, and G. M. Whitesides, "Pneumatic networks for soft robotics that actuate rapidly," *Adv. Funct. Mater.*, vol. 24, no. 15, pp. 2163–2170, 2014.

[20] E. Milana, M. Bellotti, B. Gorissen, M. De Volder, and D. Reynaerts, "Precise bonding-free micromoulding of miniaturized elastic inflatable actuators," in *RoboSoft 2019 - 2019 IEEE Int. Conf. Soft Robot.* IEEE, apr 2019, pp. 768–773.

[21] N. K. Myshkin, M. I. Petrokovets, and A. V. Kovalev, "Tribology of polymers: Adhesion, friction, wear, and mass-transfer," *Tribol. Int.*, vol. 38, no. 11-12 SPEC. ISS., pp. 910–921, nov 2005.

[22] M. Wehner, M. T. Tolley, Y. Mengüç, Y.-L. Park, A. Mozeika, Y. Ding, C. Onal, R. F. Shepherd, G. M. Whitesides, and R. J. Wood, "Pneumatic Energy Sources for Autonomous and Wearable Soft Robotics," *Soft Robot.*, vol. 1, no. 4, pp. 263–274, 2014.

[23] S. Collins, A. Ruina, R. Tedrake, and M. Wisse, "Efficient bipedal robots based on passive-dynamic walkers," *Science (80-.).*, 2005.

[24] D. J. Preston, P. Rothemund, H. J. Jiang, M. P. Nemitz, J. Rawson, Z. Suo, and G. M. Whitesides, "Digital logic for soft devices," *Proc. Natl. Acad. Sci. U. S. A.*, vol. 116, no. 16, pp. 7750–7759, apr 2019.

[25] S. T. Mahon, A. Buchoux, M. E. Sayed, L. Teng, and A. A. Stokes, "Soft robots for extreme environments: Removing electronic control," in *RoboSoft 2019 - 2019 IEEE Int. Conf. Soft Robot.*, 2019, pp. 782–787.

[26] B. Gorissen, E. Milana, A. Baeyens, E. Broeders, J. Christiaens, K. Collin, D. Reynaerts, and M. De Volder, "Hardware Sequencing of Inflatable Nonlinear Actuators for Autonomous Soft Robots," *Adv. Mater.*, vol. 31, no. 3, pp. 1–7, 2019.